Available online at www.sciencedirect.com

ScienceDirect

Ceramics International 40 (2014) 691–697

CERAMICS INTERNATIONAL

www.elsevier.com/locate/ceramint

# Optimal electroless plating rate enhancement techniques for the fabrication of low cost dense nickel/ceramic composite membranes

Amrita Agarwal, Murali Pujari, R. Uppaluri*, A. Verma

*Department of Chemical Engineering, Indian Institute of Technology Guwahati, Guwahati 781039, Assam, India*

Received 17 May 2013; received in revised form 14 June 2013; accepted 14 June 2013
Available online 24 June 2013

**Abstract**

Addressing combinatorial plating characteristics for dense metal ceramic composite membranes, this article attempts to identify the most suitable electroless plating rate enhancement technique. The support morphology considered for this work corresponds to low combinations of pore size and porosity. Cases considered for comparative assessment include conventional electroless plating (CEP), surfactant induced electroless plating (SIEP) and sonication induced electroless plating (SOEP). BET, FTIR, XRD, FESEM and nitrogen permeation techniques were employed for surface and physical characterization. It was observed that with SIEP the average metal film thickness was about 18.3 μm and with SOEP it was 24.6 μm. Correspondingly it was also observed that for SIEP baths the ratio of percent pore densification (PPD) to metal film thickness ($\delta$) i.e. PPD/$\delta$ varied from 11.2 to 5.35 and for SOEP baths PPD/$\delta$ varied from 3.5 to 4.7 for 8–24 h of sequential plating. Thereby, it was inferred that SIEP possessed maximum potential towards dense metal ceramic composite membrane fabrication for the realization of maximum PPD with minimal metal film thickness.


*Keywords:* E. Membrane; Ceramic; Surfactant; Densification

## 1. Introduction

Metal composite membranes have numerous applications such as $TiO_2$ recovery from waste water streams [1], asymmetric supports for dense palladium composite membranes [2], production of ultrapure gases for special applications [3] and hydrogen separation [4]. Presently companies involved in fabricating composite membranes for various industrial applications include Mykron, Entegris and Mott Corporation.

Amongst several fabrication processes, electroless plating (ELP) offers a good number of advantages such as uniformity in deposition irrespective of shape and size, simple experimental setup, scalability, minimal usage of electrical power, applicability for deposition on internal surfaces, edges, irregular and complex shapes, etc.

The autocatalytic metal electroless plating process is an extremely slow process and therefore plating rate enhancement techniques were explored to enhance the plating rate. However, the quality of plating remained a central issue for which plating rate enhancement techniques and their associated parameters need to be optimized. Several plating rate enhancement techniques include agitation (in the form of either membrane stirring [5] or gas sparging [6]), vacuum [7], hydrothermal [8], sonication [8] and surfactant assisted electroless plating baths [9]. However, amongst these techniques, from the perspectives of combinatorial plating characteristics and ease of operation, sonication and surfactant remained attractive, as industrial scale sonication baths are available and surfactant assisted electroless plating could be scaled up easily. Even amongst these two, surfactant induced electroless plating has significant number of features. The usage of surfactant is advantageous in two ways—firstly surfactant reduces the surface tension of the gas bubble and therefore enables the generation of smaller bubbles on the surface thereby minimizing the pitting effect. Secondly since gas bubbles are removed at a faster pace, the redox reaction shifts to the forward direction and therefore metal plating is enhanced [9]. Further

*Corresponding author. Tel.: +91 361 2582260; fax: +91 361 2582291.
*E-mail address:* ramgopalu@iitg.ernet.in (R. Uppaluri).

0272-8842/$ - see front matter © 2013 Elsevier Ltd and Techna Group S.r.l. All rights reserved.
http://dx.doi.org/10.1016/j.ceramint.2013.06.056

**Nomenclature**

| | |
|---|---|
| $A_m$ | permeable area of the membrane, $m^2$ |
| $w_0$ | dry weight of the membrane before plating, g |
| $w_i$ | dry weight of the membrane after *i*th hour of plating, g |
| $w$ | total amount of nickel originally available in the plating bath, g |
| $n$ | number of plating cycles |
| $V_0$ | volume of plating solution in each plating cycle, L |
| $M_{Ni}$ | molecular weight of nickel metal, g/mol |
| $\rho_{Ni}$ | density of nickel metal, $g/cm^3$ |
| $J$ | flux through the membrane, $mol/m^2$ s |
| $\overline{J}$ | average flux through the membrane, $mol/m^2$ s |
| $i$ | hour of nickel plating (as exponent) |
| $\overline{r}_i$ | plating rate, mol/L s |
| $t_i$ | time of plating for the *i*th hour, h |
| PPD | percent pore densification, % |
| CEP | conventional electroless plating |
| ELP | electroless plating |
| SIEP | surfactant induced electroless plating |
| SOEP | sonication induced electroless plating |

ultrasonic waves in sonication induced electroless plating account for increased mass transport, interfacial cleaning and thermal effects [10].

To date, electroless plating research for metal composite membranes was primarily targeted from a product quality oriented perspective, but not from process engineering perspectives. Combinatorial plating characteristics involving the simultaneous assessment of plating process parameters (such as plating rate) and product parameters (such as average pore size, average pore densification and metal film thickness) are important areas of research that could drive the efficacy of both manufacturing processes and materials. From such a perspective for dense metal composite membranes, the literature is scarce. Further, time dependency of the plating and process characteristics and rate enhancement techniques (sonication and surfactant) for metal composite membranes were not addressed. Also in the literature, while SIEP has been studied significantly for stainless steel supports, alumina supports [11] and palladium deposition, SIEP studies toward nickel composite membranes have not been addressed for ceramic supports. Such studies are also required from a processing perspective as well, given the fact that stainless steel membranes are significantly more expensive than ceramic membranes and thus the utilization of ceramic membrane could pave the way for faster research commercialization and scaleup.

Process engineering studies toward materials fabrication need to first address compatibility of support materials towards the desired application. Deliberating towards the synchronity of process–material compatibility, our previous work addressed the preparation, characterization and optimization of a low cost ceramic support for the preparation of nickel ceramic composite membranes [12]. This work is a natural extension of such work and aims towards a critical examination of electroless plating process characteristics for the optimized support.

## 2. Experimental

Laboratory made ceramic substrates with a diameter of 36 mm and thickness of 3.5 mm fabricated at a pressure of 4.9 MPa were used as supports for the electroless plating experiments. The pore size $d_p^{sup}$ and effective porosity $(\varepsilon/q^2)$ of the substrates were about 50–70 nm and 10–15% respectively. The ceramic substrates were fabricated by the dry compaction method and sintered at 900 °C and the inorganic raw materials used for fabrication of ceramic substrate were as mentioned in Table 1.

Surface and physical characterizations were performed using a number of techniques. The BET surface area and pore size of the support material were determined by $N_2$ adsorption desorption isotherm at 77 K by using a surface area analyzer (Beckman-Coulter; Model: SA3100). Fourier transform infrared spectroscopy (FTIR) analysis was done to record the characteristic peaks of various raw materials. X-Ray diffraction (XRD) analysis of the inorganic ceramic substrate and metal membrane was conducted to evaluate the extent of phase transformations. Field emission scanning electron microscopic (FESEM) study (Make: Oxford; Model: LEO 1430VP, UK) was carried out to analyze the presence of possible defects and estimate the membrane pore size. The estimation of average membrane pore size from FESEM micrographs was carried out using ImageJ software. The effective porosity of the membrane was evaluated by weight gain method with water as the wetting liquid. Nitrogen permeation experiments were conducted to quantify membrane morphological parameters such as flux of the composite membranes and average pore size ($d_p$) that contribute to the transport and the experimental procedure was similar to the one as discussed in our previous work [12].

### 2.1. Electroless plating

Typical composition for nickel electroless plating technique is summarized in Table 2. Prior to plating, the substrates were seeded with the conventional procedure of activation and sensitization with palladium seeds. Eight sequential 1 h nickel deposition steps with a nickel concentration of 0.08 mol/L, loading ratio

Table 1
Composition of raw materials of ceramic membrane supports.

| Material | Composition on dry basis (wt%) |
|---|---|
| Kaolin | 40 |
| Feldspar | 15 |
| Quartz | 15 |
| $Na_2CO_3$ | 10 |
| Pyrophyllite | 10 |
| Boric acid | 5 |
| Sodium metasilicate | 5 |

of 203 $cm^2$/L, 50% excess hydrazine hydrate (reducing agent) and plating bath temperature of 80 °C were used to yield the nickel composite membranes.

Five different membranes as mentioned in Tables 3 and 4 were focused for the development of nickel composite membranes. Prior to plating, raw membranes $M_4$ and $M_5$ were treated. The treatment involved immersion of the support in an alkaline (NaOH) solution which modified the support morphology and the pore diameters increased from 50–70 nm to 90–120 nm as discussed in detail in our previous work [12].

### 2.2. Evaluation of plating characteristics

The process and plating parameters for evaluating the performance of various electroless plating baths for fabricating dense nickel membranes are average trans-membrane flux $\overline{J}$, average plating rate ($\overline{r}_i$), average thickness of the nickel layer ($\delta$) and percent pore densification PPD (%). Average trans-membrane flux and PPD calculations were similar to our earlier reported work [12].

Table 2
Typical composition of conventional and surfactant induced nickel electroless plating baths.

| S. no. | Component | Amount |
|---|---|---|
| 1 | Nickel sulfate | 0.08 mol/L |
| 2 | Hydrazine hydrate | 50% excess |
| 3 | Trisodium citrate | 0.2 mol/L |
| 4 | Sodium hydroxide | 10–12 |
| 5 | Cetyltrimethylammonium bromide | 1.2 g/L |

Table 3
Summary of various cases investigated for the development of nickel composite membranes.

| Case | Type of support | Type of ELP |
|---|---|---|
| $M_1$ | Raw | Conventional |
| $M_2$ | Raw | Sonication |
| $M_3$ | Raw | Surfactant |
| $M_4$ | Treated | Surfactant |
| $M_5$ | Treated | Sonication |

Table 4
Ratio of plating rate with respect to the base case (CEP).

| Type of plating | Ratio of plating rate | | |
|---|---|---|---|
| | 8 h | 16 h | 24 h |
| SOEP ($M_2$) | 9.97 | 6.18 | 3.82 |
| SIEP ($M_3$) | 6.31 | 3.22 | 2.25 |
| SIEP ($M_4$) | 13.98 | 6.21 | 3.41 |
| SOEP ($M_5$) | 16.62 | 6.97 | 4.58 |

Starting taken as 40 h for CEP ($M_1$).

The theoretical nickel film thickness ($\delta$) was evaluated using the weight gain method and was expressed as follows:

$$\delta = \frac{w_i - w_0}{\rho_{Ni} A_m} \quad (1)$$

where $\rho_{Ni}$ $\left(g/cm^3\right)$ represents the density of nickel metal and $A_m$ ($m^2$) the membrane surface area for nitrogen permeation experiments. The plating rate $\overline{r}_i\left(\text{mol}/(\text{L s})\right)$ was evaluated as follows:

$$\overline{r}_i = \frac{w_i - w_0}{M_{Ni} n V_0 t_i} \quad (2)$$

where $t_i$ corresponds to the time of plating for the $i$th hour.

## 3. Results and discussions

### 3.1. Surface characterization

The BET surface area of support was 2.712 $m^2$/g and total pore volume was 0.0156 ml/g with no micropore volume. The average pore size as evaluated from Barrett–Joyner–Halenda (BJH) pore volume distribution was found to be 35 nm similar to our previous addressed work [12]. Similarly the Fourier transform infrared spectra recorded characteristic peaks of kaolin for the raw material and after sintering of the raw material mixture at 900 °C were assigned to C–H bonds, C═C bonds, Si–O–Al and Si–O bonds as discussed earlier in detail [12].

X-Ray diffraction phase analysis was done using the ICDD-JCPDS database. Fig. 1 presents the XRD patterns of raw material mixture, sintered ceramic support, and the nickel membrane. The phases for kaolin, quartz and sodium carbonate appeared in the raw material mixture as reported earlier [12]. Further on sintering it was also observed that the peak corresponding to kaolin disappeared due to the transformation of kaolinite to metakaolinite and that corresponding to sodium

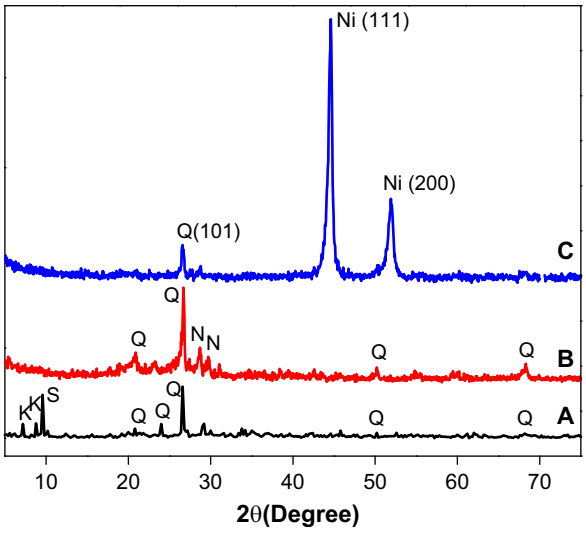


Fig. 1. XRD patterns for (i) A—raw material, (ii) B—sintered support and (iii) C—nickel plated membrane ($M_4$) where K signifies kaolin, S—sodium carbonate, Q—quartz, N—Nephiline and Ni—nickel.

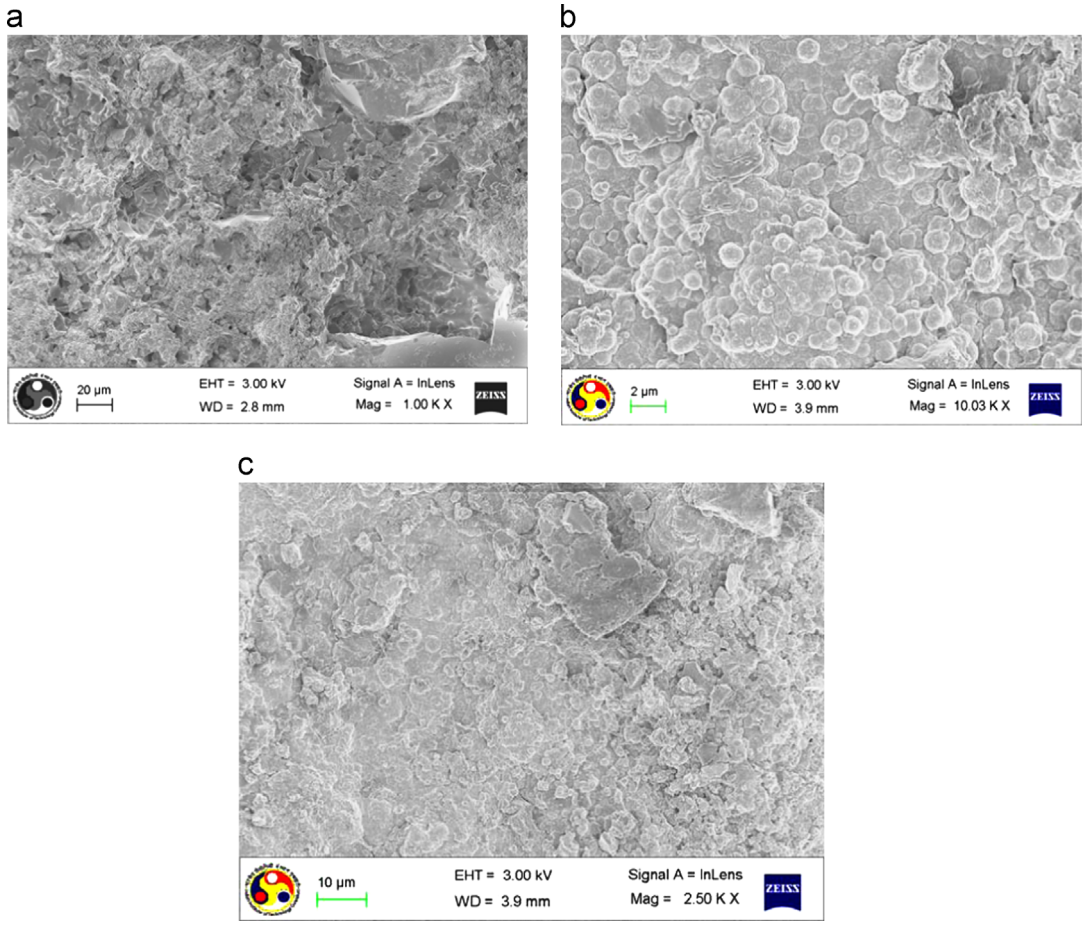


Fig. 2. Surface FESEM micrographs of (a) ceramic treated support, (b) nickel membrane fabricated with SIEP process ($M_4$) and (c) nickel membrane fabricated with SOEP process ($M_5$).

carbonate disappeared due to thermal decomposition. The new phase that appeared in the XRD pattern on sintering was Nephiline ($Na_2O$, $Al_2O_3$, $2SiO_2$) which was produced by the reaction of sodium oxide ($Na_2O$) and metakaolinite at temperature around 800 °C [13]. Moreover the diffractogram graphs after sintering (profile B) indicated no change in the quartz peak trends thereby implying that quartz phase was not at all affected by sintering of inorganic materials within the studied temperature range considered in this work. The metallic nickel peaks for electroless plating (profiles C) appeared at diffraction angle $2\theta = 44.5^\circ$ and $51.8^\circ$ due to the diffraction of (111) and (200) planes [Pdf no. 00-004-0850]. Further, temperature programmed reduction analysis (Model: Chemisorb 2720; Make: Micrometrics) was also conducted for the nickel plated membrane and no reduction peak was observed indicating that only metallic nickel was deposited on the ceramic substrate.

Fig. 2 presents the surface FESEM micrographs of the ceramic substrate and nickel layer deposited with an initial nickel sulfate concentration ($C_i$) of 0.08 (mol/L) after 12 h of sequential plating with SIEP and SOEP processes. The nickel particles were uniformly dispersed as observed on the surface. Further it was observed that SIEP process showed better surface finish with agglomerates, thereby providing faster densification with lesser pinholes as desired. Average pore size analysis of the ceramic substrate done using ImageJ software gave an average pore size of 150 nm which was close to that evaluated from nitrogen permeation experiments (90–120 nm).

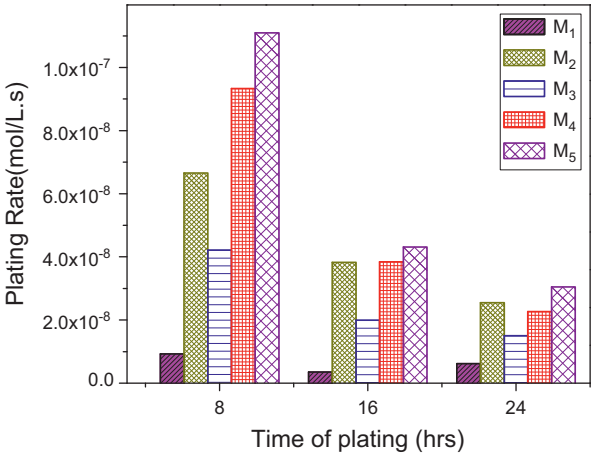


Fig. 3. Variation of plating rate with time of plating.

### 3.2. Plating rate

Fig. 3 presents the trends for fluctuation in plating rate with respect to time of plating. It was observed that the plating rates for $M_1$ varied from $6.68 \times 10^{-9}$ to $6.58 \times 10^{-9}$ (mol/L s), for $M_2$ from $6.65 \times 10^{-8}$ to $2.54 \times 10^{-8}$ (mol/L s), for $M_3$ from $4.2 \times 10^{-8}$ to $1.5 \times 10^{-8}$ (mol/L s), for $M_4$ from $9.3 \times 10^{-8}$ to $2.2 \times 10^{-8}$ (mol/L s) and for $M_5$ from $11.1 \times 10^{-8}$ to $3.58 \times 10^{-8}$ (mol/L s). Further, Table 3 illustrates the ratio of plating rate with respect to the base case (CEP). From the data it was analyzed that for both the cases of treated ($M_5$) and raw supports ($M_2$), SOEP membranes gave higher plating rate when compared to both CEP and SIEP. Such data trends are also in agreement to Wu et al. [14] who inferred that introduction of ultrasonic waves during electroless nickel deposition enhances the plating rate.

As compared to Bulasara et al. [15] who reported a CEP rate of $1.51 \times 10^{-6}$–$9.79 \times 10^{-6}$ (mol/L s) for an average pore size of 275 nm, porosity of 0.44 and varying stirrer speed, our work indicated a lower plating rate of $6.68 \times 10^{-9}$ (mol/L s). Therefore, it was inferred that plating rate was strongly influenced by average pore size and porosity and hence plating rate enhancement techniques became predominantly significant to influence the quality of plating characteristic for the supports considered for this work.

Experimentally it was reported that the plating rate and the quality of plating were optimal for supports within the pore size of 250–300 nm and porosity of 35–50% [16]. This work referred to the performance characteristics of a low cost ceramic membrane that was characterized with even lower combinations of pore size (90–120 nm) and effective porosity (10–15%). From metal film densification perspective, a support with lower pore size and porosity enabled faster densification but did not provide good adhesion of the metal film to the support. On the other hand, a support with higher pore size and porosity required thicker dense metal films to achieve dense composite membranes [17] with good adhesion strength.

Therefore, the metal densification perspective shall not be regarded from the perspective of achieving only thin dense metal film thickness, as the mechanical strength of the film was also of paramount importance. Therefore, further research was required to identify optimal membrane pore size and porosity values that enabled achieving stable dense metal films on the surface. Nonetheless, the role of plating rate enhancement techniques to alter the strength related properties could not be ignored in this context.

### 3.3. Film thickness

Fig. 4 reports the data trends for increment in metal film thickness with time of plating. It was observed that for 8–24 h of nickel plating, the metal film thickness increased from 0.8 to 5 μm for $M_1$ (CEP), 6–20.5 μm for $M_2$ (SOEP), 3.7–12.1 μm for $M_3$ (SIEP), 8.4–18.3 μm for $M_4$ (SIEP) and 9.9–24.6 μm for $M_5$ (SOEP). Further, it was observed that the nickel film plating rate was 1 μm/h for the SIEP baths which was 10 times higher than the value for CEP baths (0.1 μm/h). Subsequently it was observed that the nickel film plating rate was 1.2 μm/h for the sonication assisted baths. Literature indicated that the corresponding plating rates for a macroporous support were 1.9, 1.8 and 3.1 μm/h for CEP, SIEP and SOEP respectively [15]. While the desired objective is to achieve a dense nickel film on the surface of the porous ceramic support, it was observed that the first few plating steps enabled the deposition of nickel film inside the support pores which would facilitate good bonding between the support and the metal film. In addition, further insights to gain information related to the uncertainities associated to theoretical metal film thickness have not been obtained using FESEM cross section images, as Bulasara et al. [18] have indicated that the theoretical thickness values are as good as those measured using the FESEM image analysis.

Thus sonication resulted in tremendous increase in film thickness due to simultaneous increase in both deposition rate and plating efficiency for both the treated and the untreated supports. These observations are in agreement with Kathirgamanathan [19] who concluded that sonication enhanced metal deposition and improved adhesion of the metal to the membrane

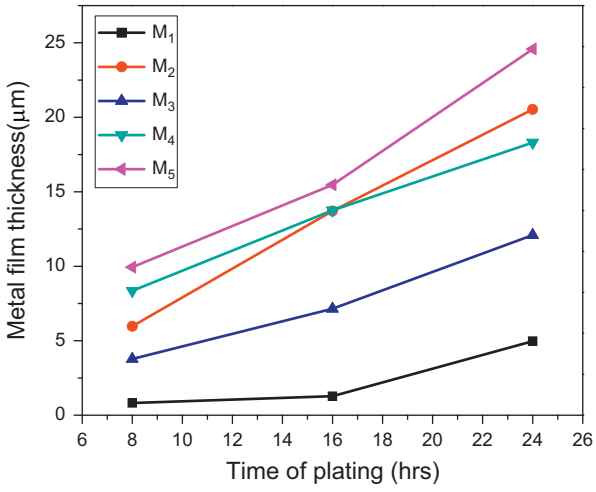


Fig. 4. Variation of film thickness with time of plating.

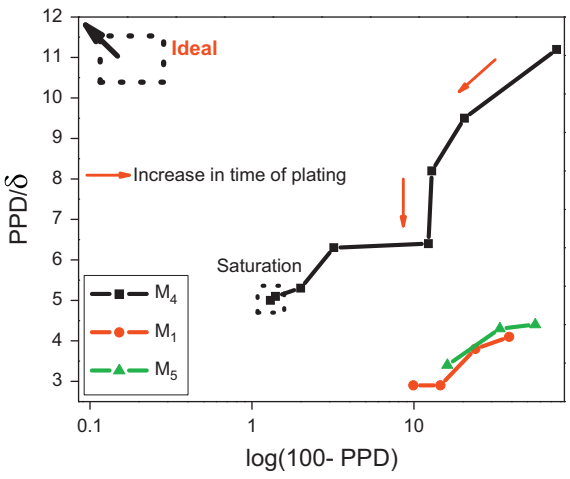


Fig. 5. PPD/$\delta$ vs. log(100−PPD) tradeoffs.

surface. Similar conclusions were inferred by Ilias et al. [20] through their statement that the same thickness could be obtained by reducing the plating time if a suitable surfactant was used during electroless plating.

### 3.4. Efficacy of mass transfer enhancement

Fig. 5 presents the time dependent variation of (100−PPD) and PPD/$\delta$ values for nickel composite membrane fabricated by various rate enhancement techniques. The graph corresponds to conceptual extensions of the measured data to visualize the extent of pore densification ($x$-axis) with respect to the amount of metal required to densify the pores ($y$-axis). Conceptually, an ideal electroless plating process supplemented with optimal rate enhancement technique should achieve maximum PPD/$\delta$ and minimal (100−PPD) values and therefore should refer to the values closely located to the $y$-axis. From the figure, it is observed that PPD values varied from 26% to 90% and PPD/$\delta$ from 2.2 to 2.86 in 32–64 h of rigorous plating experimentation for $M_1$. Further, PPD values varied from 34.9% to 83.9% and PPD/$\delta$ values from 3.5 to 4.7 for $M_5$ after 24 h of sequential plating. However, for the same time of plating, PPD values varied from 24% to 98% and PPD/$\delta$ values from 11.2 to 5.35 were obtained for the surfactant assisted baths ($M_4$). Therefore from membrane pore densification perspective, surfactant assisted electroless plating yields the best possible conditions of nickel metal deposition on the membrane surface and corresponds to a combinatorial performance characteristics of 98.7% PPD and PPD/$\delta$ value of 4.98 for a nickel composite membrane with a film thickness ($\delta$) of 19.8 μm after 32 h of rigorous experimentation.

Further, it was observed that there exists a saturation point for membrane $M_4$, as there was no significant improvement in the PPD value (from 98% to 98.7%) from 24 to 32 h of sequential deposition. The saturation phase in the plating period was represented by a sharp reduction in the length of the consecutive points. However, the case did not correspond to 100% saturation, which should have been indicated by a vertical straight line in the graph. Since PPD could not be altered much with the prevalent conditions, an interesting issue for further research was to examine the role of solution concentrations (metal or reducing agent concentration or both) as well as the mode of contacting to bypass the saturation phase and continue the plating process to ensure that 100% densification could be achieved.

If we consider the case which has comparatively higher values of PPD and lower time of plating, the only feasible option was for surfactant induced electroless plating as shown in Fig. 5. A PPD value of about 98% along with the experimental inference of porous membranes presumably indicated that the utilization of supports with lower surface pore sizes could yield a dense nickel/ceramic composite membrane in about 24–32 h of sequential electroless plating steps at lower metal concentration (0.08 mol/L). Further, it can be stated that although sonication improved the plating rate and metal film thickness, it did not provide significant reduction in pore size as compared to surfactant induced electroless plating.

The efficient design of electroless plating process needs to maximize percent pore densification (PPD) and minimize the metal film thickness ($\delta$). This work also recognized the immediate need to identify suitable mass transfer enhanced electroless plating processes that could provide good combinations of PPD and film thickness ($\delta$). The approach presented in this work could be used as a new methodology for the assessment of nickel electroless plating baths with variant morphological parameters and conditions of operations.

Thus surfactant techniques were observed to be more effective to enhance the PPD values significantly close to 100% as shown clearly in Fig. 5. This is also in agreement with the work of Islam et al. [21], who inferred that dense and thinner films could be formed with shorter deposition time using SIEP method. A possible reason for not achieving 100% PPD was that beyond a particular point the solution concentration imposes limitations on the quality of plating.

## 4. Conclusions

This work elaborated upon engineering research approaches and experimental methodologies required for the cost effective fabrication of nickel/ceramic composite membranes for electroless plating processes. It could further be extended towards palladium composite membranes and multi-metal membranes that have functional applications as efficient gas separating devices. Emphasis was primarily towards the efficacy of various rate enhancement techniques that could be supplemented to electroless plating process for the fabrication of dense metal/ceramic composite membranes. Most importantly, this work showed that sonication did not contribute to 100% pore densification for the chosen support, even though sonication contributed to enhanced nickel deposition rate substantially. This work reported time dependent performance of electroless plating baths for nickel/ceramic composite membrane fabrication which promoted further insights in the metal deposition characteristics such as variation in thickness, PPD and average pore size with time of deposition. Thereby, this work featured the minimal number of plating steps required to achieve desired membrane characteristics. Interesting feature of such research was to examine the compatibility of nickel films in terms of adhesion during electroless plating. The conceptual insights gathered in this work required further refinement and fine tuning towards assessing the role of better quality porous supports in combinatorial performance characteristics of electroless plating baths.

The experimental investigation confirmed that nickel deposition on non-conducting surfaces was an extremely slow process and efforts were required to enhance the plating rate as well as the quality of deposition of metal on non-conducting surfaces. The stagnation of time dependent PPD profiles needed further experimental investigation and careful contacting of reducing agent with metal precursors to substantially enhance PPD and could not be ruled out. This was especially evident from time dependent nickel PPD profiles in the later

stages of plating. Optimization of conditions that drive away the achievement of saturation in product quality would require sophisticated process modification. For example a time dependent variable frequency sonicator may provide better PPD profiles or good quality of plating. Further, SIEP was exceptionally good to achieve highest values of PPD/$\delta$ for the membranes. Thus, it could be concluded that SIEP possessed maximum potential towards metal ceramic composite membranes and would be investigated substantially to improve the quality of plating.

This work emphasized upon the criticality of mass transfer enhancement to accommodate morphological parametric features to achieve dense metal ceramic composites. It exclusively focused upon the quality of deposition (PPD profiles) using supports with lower pore sizes. It appeared that SIEP was the most promising action in terms of economics, simplicity, ease of operation and quality of deposition as the technique enabled the realization of maximum value of PPD/$\delta$. Further research was anticipated with respect to metal concentration since the plating rate increased with metal solution concentration and decreased with loading ratio. Higher conversions without jeopardizing the PPD variation with SIEP need to be studied and will be taken up as the future work.

## Acknowledgments

This work is partially supported by a grant from the DST (Department of Science and Technology), New Delhi. Any opinions, findings and conclusions expressed in this paper are those of the authors and do not necessarily reflect the views of DST, New Delhi. Special thanks to Dwipjyoti Saloi who worked as project assistant and helped us for this work.

## References

[1] S. Jha, K.L. Rubow, Nickel microfiltration media for gas and liquid filtration, Advances in Filtration and Separation Technology 13 (1999) 512–520.
[2] W.H. Lin, Y.C. Liu, H.F. Chang, Autothermal reforming of ethanol in a Pd–Ag/Ni composite membrane reactor, International Journal of Hydrogen Energy 35 (2010) 12961–12962.
[3] S.K. Ryi, J.S. Park, S.J. Park, D.G. Lee, S.H. Kim, Fabrication of nickel filter made by uniaxial pressing process for gas purification: fabrication pressure effect, Journal of Membrane Science 299 (2007) 174–180.
[4] B. Ernst, S. Haag, M. Burgard, Permselectivity of a nickel/ceramic composite membrane at elevated temperatures: a new prospect in hydrogen separation?, Journal of Membrane Science 288 (2007) 208–217
[5] M.E. Ayturk, Y.H. Ma, Electroless Pd and Ag deposition kinetics of the composite Pd and Pd/Ag membranes synthesized from agitated plating baths, Journal of Membrane Science 330 (2009) 233–245.
[6] O. Altinisik, M. Dogan, G. Dogu, Preparation and characterization of palladium plated porous glass for hydrogen enrichment, Catalysis Today 105 (2005) 641–646.
[7] S.E. Nam, S.H. Lee, K.H. Lee, Preparation of a palladium alloy composite membrane supported in a porous stainless steel by vacuum electrodeposition, Journal of Membrane Science 153 (1999) 2163–2173.
[8] V.K. Bulasara, M.S. Abhimanyu, T. Pranav, R. Uppaluri, M.K. Purkait, Performance characteristics of hydrothermal and sonication assisted electroless plating baths for nickel–ceramic composite membrane fabrication, Desalination 284 (2012) 77–85.
[9] B.H. Chen, L. Hong, Y. Ma, T.M. Ko, Effects of surfactants in an electroless nickel-plating bath on the properties of Ni–P alloy deposits, Industrial and Engineering Chemistry Research 41 (2002) 2668–2678.
[10] I. Haas, A. Gedanken, Sonoelectrochemistry of $Cu^{2+}$ in the presence of cetyltrimethylammonium bromide: obtaining CuBr instead of copper, Chemistry of Materials 18 (2006) 1184–1189.
[11] L.L.O. Silva, D.C.L. Vasconcelos, E.H.M. Nunes, L. Caldeira, V.C. Costa, A.P. Musse, S.A. Hatimondi, J.F. Nascimento, W. Grava, W.L. Vasconcelos, Processing, structural characterization and performance of alumina supports used in ceramic membranes, Ceramics International 38 (2012) 1943–1949.
[12] A. Agarwal, M. Pujari, R. Uppaluri, A. Verma, Preparation, optimization and characterization of low cost ceramics for the fabrication of dense nickel composite membranes, Ceramics International (2013), http://dx.doi.org/10.1016/j.ceramint.2013.03.024.
[13] M.C. Wang, N.C. Wu, M.H. Hon, Preparation of nepheline glass–ceramics dental porcelain, Materials Chemistry and Physics 37 (1994) 370–375.
[14] Z. Wu, S. Ge, M. Zhang, W. Li, K. Tao, Synthesis of nickel nanoparticles supported on metal oxides using electroless plating: controlling the dispersion and size of nickel nanoparticles, Journal of Colloid and Interface Science 330 (2009) 359–366.
[15] V.K. Bulasara, R. Uppaluri, H. Thakuria, M.K. Purkait, Combinatorial performance characteristics of agitated nickel hypophosphite electroless plating baths, Journal of Materials Processing Technology 211 (2011) 1488–1499.
[16] M. Kitiwan, D. Atong, Effects of porous alumina support and plating time on electroless plating of palladium membrane, Journal of Materials Science and Technology 26 (2010) 1148–1152.
[17] I.P. Mardilovich, E. Engwall, Y.H. Ma, Dependence of hydrogen flux on the pore size and plating surface topology of asymmetric Pd-porous stainless steel membranes, Desalination 144 (2002) 85–89.
[18] V.K. Bulasara, H. Thakuria, R. Uppaluri, M.K. Purkait, Effect of process parameters on electroless plating and nickel–ceramic composite membrane characteristics, Desalination 268 (2011) 195–203.
[19] P. Kathirgamanathan, Ultrasound-assisted electroless deposition of copper onto and into microporous membranes for electromagnetic shielding, Polymer Communications 35 (1994) 430–432.
[20] S. Ilias, M.A. Islam, Fabrication of Pd/Pd-alloy Films by Surfactant Induced Electroless Plating for $H_2$ Separation from Advanced Coal Gasification Processes, Patent Application #20100068391 (USPTO assignment date: March 18, 2010).
[21] M.S. Islam, M.M. Rahman, S. Ilias, Characterization of Pd–Cu membranes fabricated by surfactant induced electroless plating (SIEP) for hydrogen separation, International Journal of Hydrogen Energy 37 (2012) 3477–3490.